A98-31660

ICAS-98-5,10,2

EULER/NAVIER-STOKES SIMULATION FOR PROPULSION-AIRFRAME INTEGRATION OF ADVANCED PROPELLER-DRIVEN AIRCRAFT IN THE EUROPEAN RESEARCH PROGRAMS GEMINI/APIAN

M. Amato[1]
CIRA, Centro Italiano Ricerche Aerospaziali, Via Maiorise, 81043 Capua (CE), Italy

F. Boyle[2], J.A. Eaton[3],
National University of Ireland, Galway, Ireland

P. Gardarein[4]
ONERA, BP 72 92322 Chatillon Cedex, France

Abstract

Power plant design and installation are critical factors in the design and realisation of competitive aircraft. The synergetic and integrated use of experimental and numerical techniques is mandatory to effectively design new aeroplanes. The propulsion-airframe integration is the subject of various EC funded projects. In this paper, the GEMINI II and APIAN projects are described; the topic area is the propulsion-airframe integration for a generic propeller driven regional commuter flying in transonic conditions. The main focus of this paper is on a discussion of the CFD activities realised within these projects and obtained results. These activities are as follows: isolated propeller aerodynamic analysis; actuator disk modelling; wing installation effects on propeller aerodynamics; aerodynamic prediction of the flow about a fuselage-wing-nacelle configuration with propeller slipstream simulation. A comparison of some computed and experimental results for the GEMINI II models are presented. These results clearly show the capability of analysing the problems related to propulsion-airframe integration.

Introduction

Aerodynamic and structural design of new competitive aircraft for civil and military aviation nowadays is one of the most challenging activities. Environmental issues such as fuel consumption and noise emission (i.e. environmental compatibility) together with performance, safe operation, favourable flight handling, weight, maintainability, manufacturing, and costs are of vital importance for the success of a new aircraft.

Proper engine design and propulsion-airframe integration are determinant elements to ensure these factors. This is true for both turboprop and turbofan power plants: the former with the new heavily loaded high speed propellers introduce perturbations that have to be taken into account in the overall design process; for the latter the ever-growing by-pass ratio has dictated an increase of the engine's diameter causing problems of installation and related drag that can overwhelm the larger efficiency of the new propulsion systems.

The synergetic and integrated use of experimental and numerical techniques is mandatory to effectively design new competitive aircraft. As well as being used as a tool integrated with experimental techniques for aircraft design, CFD should be seen as an analysis tool to support wind tunnel tests. With respect to the latter point, CFD allows us to: verify model installation; identify special flow features before the wind tunnel testing, and hence to concentrate measurements in specific areas of interest; check model loads;

1 Senior Researcher, Head CFD Unit
2 Doctoral Candidate, Dept. of Mechanical Engineering
3 Director, Aerospace Research Unit
4 Senior Researcher, Applied Aerodynamics Department

21st ICAS Congress
13-18 September 1998
Melbourne, Australia

perform comparisons of computed and measured data.

The propulsion-airframe integration problem and experimental and numerical techniques necessary to analyse this topic have been the subject of various EC BRITE/EURAM funded projects since 1990. Examples of such projects are GEMINI, GEMINI II, APIAN, DUPRIN, DUPRIN II, ENIFAIR.

In this work, some CFD activities carried out within GEMINI II and in progress within APIAN (those performed by CIRA, NUIG and ONERA) are described and an overview of numerical results and their comparison with experimental data is presented. The wind tunnel experiments and results are discussed in a complementary paper [1].

The following CFD activities and results will be discussed: isolated propeller aerodynamic analysis; actuator disk modelling; wing-installation effects on propeller aerodynamics; aerodynamic prediction of fuselage-wing-nacelle and wing-nacelle configurations with propeller slipstream simulation.

The isolated propeller modelling has been performed via two different steady Euler solvers, and the results are compared with experimental data. Furthermore, the wing installation effect on the propeller aerodynamics has been checked by a pseudo-unsteady (averaged) simulation.

The averaged results of the isolated propeller simulations have been employed to assemble the data needed for the actuator disk boundary conditions. This actuator disk modelling has been applied in the steady flow simulation of both the isolated configuration and of the fuselage-wing-nacelle model. The actuator disk results for the isolated configuration are compared with the averaged steady results around the isolated propeller-blade geometry.

Steady results for the fuselage-wing-nacelle and wing-nacelle models at different Mach numbers and angles of attack are discussed and compared with wind tunnel results.

The GEMINI / APIAN Projects

In 1990 the GEMINI project was launched by the EC within the BRITE/EURAM Programme. GEMINI is an acronym for "Basic test rig for a **GE**neric **M**odel for tunnel test on Airframe Propulsion **In**tegration with emphas**I**s on Advanced Propellers". The aim of this project was the specification and design of a large modular wind tunnel model to investigate propulsion-airframe integration problems for a generic regional commuter. The model would be powered by air turbines for engine simulation.

The GEMINI II project started in 1993 following the successful conclusion of GEMINI. The GEMINI II project, funded by the EC within the III BRITE/EURAM Framework, was coordinated by Aerospatiale and the project team was comprised of Alenia, CASA, CIRA, Dornier, ONERA, NLR, Ratier Figeac, National University of Ireland Galway (NUIG, former UCG), ARA, and AirTechnologies. GEMINI II focused on the investigation of the aerodynamic interactions between a propeller slipstream and a typical 50 seater airframe at transonic speeds (Mach=0.72). The objectives of the project were: the development of wind tunnel models with turbo propeller simulators; the enhancement of methodologies and tools for the execution of wind tunnel tests with turbo powered models; the completion of wind tunnel experiments to investigate aerodynamics of propeller to airframe interaction; the development and validation of aerodynamic prediction tools.

In parallel, another project, SNAAP, was running with the aim of studying the aeroacoustic behaviour of isolated high speed propellers (up to M=0.78). Wind tunnel experiments were performed and a large data base of acoustic and aerodynamic data was created. Furthermore, theoretical tools for aeroacustic prediction were developed and correlated with experimental results.

A new project, APIAN, started in 1996 in the wake of the results achieved in GEMINI II and SNAAP. APIAN is an acronym for "**A**dvanced **P**ropulsion **I**ntegration for **A**erodynamics and **N**oise". This project is focused on advanced propeller-driven aircraft equipped with high-speed propellers. The main objectives of the project are: the enhancement of the wind tunnel model developed during the GEMINI projects with the addition of high-lift devices, thus exploiting of the modularity of the model; the completion of experiments to investigate the aerodynamics and acoustics of high-speed propellers and the interaction with the airframe; the development and validation of aerodynamic prediction tools.

These European projects represent a join effort by the major European industries producing propeller-driven aircraft with the related national research institutes and a national university in order to enhance the knowledge about the physical and engineering problems related to propulsion-airframe integration and to develop

and improve the tools necessary to investigate such problems.

Wind Tunnel Tests

The GEMINI II wind tunnel tests and models are briefly described; for more detailed information the reader is referred to a related paper [1].

The tests were performed on 1/8th scale models: an isolated propeller configuration, and a fuselage-wing-nacelle-propeller model (installed configuration). The isolated propeller model consisted of : six carbon fibre blades, a hub, a spinner, a minimum body (containing the pressure-driven turbine), and the instrumentation. In the installed configuration the fuselage is made up of three parts: a front part comprised of a cockpit and a cylindrical part; a central part to which the wings are attached; and a rear part where the rear sting is connected. The model is motorised with two propellers consisting of six carbon fibre blades, each driven by a turbine fed with compressed air. Both propellers were tested in the isolated set up. The models were instrumented with rotating shaft and fixed balances; on the installed configuration about 300 pressure taps were distributed.

Isolated propeller tests were performed in the ONERA S1MA wind tunnel; CASA was in charge of the experiments. The propeller was monitored by two balances; a six components fixed balance and a rotating balance. A slipstream survey was carried out and a data comparison between the readings from the two balances showed excellent agreement.

The installed tests were also carried out in the ONERA S1MA wind tunnel; CASA was in charge of the experiments again. Tufts, installed on the wing upper surface and on the outboard side of the nacelle, showed a separation at very low Mach numbers on the rear part of the nacelle. In the " propeller on " configuration two blade settings were tested and a comparison between port and starboard propellers was accomplished.

The Theoretical Task

The CFD activities performed by CIRA, ONERA, and NUIG within GEMINI II are summarised here.

The CFD task is split in two sub-tasks: propeller aerodynamics (NUIG, ONERA), and airframe aerodynamics (CIRA, Dornier, Alenia).

The main objectives for the propeller sub-task are: the investigation of state-of-the-art methodologies for the computation of the unsteady flow field around an isolated propeller at non-zero angle of incidence (NUIG); the computation of the steady and unsteady flow around the wind tunnel isolated propeller configuration (NUIG, ONERA); the generation of actuator disk models of the isolated propeller (NUIG, ONERA); a direct computation of the mutual interaction between wing and propeller (ONERA); a comparison of measured and computed data for the isolated propeller (NUIG, ONERA). The actuator disk models are used by the airframe group (CIRA, CASA, DASA-Dornier) in their aerodynamic calculations of the flow fields about fuselage-wing-nacelle and wing-nacelle power-on configurations.

The main objectives for the airframe sub-task are: the development and validation of aerodynamic prediction tools; the prediction of the flow field around the airframe, including the propeller slipstream modelling, for the safe preparation of the wind tunnel tests; the identification of special flow features before the wind tunnel testing, and to enable the concentration of measurements in specific areas of interest; the correlation of computed and measured data; the enhancement of the knowledge about the physical and engineering problems related to propulsion-airframe integration.

Steady Isolated Propeller Flow Field Calculations

The Euler simulations of the flow field around the propeller blades at zero-incidence inflow-angle performed by NUIG and ONERA are described here.

ONERA code

The CANARI code [2] is a 3D solver for the Euler equations and for the averaged Navier-Stokes equations associated with a turbulence model. Used at ONERA and by manufacturer, as well for aircraft as for turbo-machinery configurations, CANARI is based on a cell-centred multi-domain finite volume approach. All types of structured grids can be mixed together, with adjacent or overlapping domains. This multi-domain approach combined with the multiple application are key characteristics which allow the treatment of various configurations, especially by easing the mesh generation for complex industrial configurations. Acceleration techniques including implicit residual smoothing and local time stepping are used to speed up the convergence of the central scheme. For the propeller applications a specific version of the solver is used, the equations being written with absolute variables

instead of relative variables in order to avoid numerical problems far away from the propeller where a uniform free stream condition is applied. Due to periodic properties of the isolated propeller flow field at zero incidence inflow angle, only a blade to blade interval is computed with node coincidence at the periodic boundaries. This grid has 130x30x50 (121,440) points (respectively in axial, tangential and radial directions) with 546 points on each blade surface. The grid lines are refined in root and tip region (r/Rtip=1). The "H" grid topology eases node coincidence and allow also to keep planar upstream and downstream boundaries perpendicular to the rotation axis. In addition, in order to provide actuator disk data, constant radius lines are used in tangential direction, in order to avoid interpolation when the 3D flow field is averaged in circumferential direction for the actuator disk models needed for the aircraft computations. The propeller option of CANARI code was used in Euler mode for the GEMINI II propeller computations. Convergence of the results was obtained after 1000 implicit iterations, with a decrease of more than 3 orders of magnitude on the maximum density residual.

NUIG code

A three-dimensional compressible Euler finite-volume code[3] is used to predict the steady inviscid flow field around the isolated propeller at zero angle of incidence. The appropriate free stream conditions and propeller operating conditions are specified in an analysis input file. The Euler code solves the integral equations of the conservation of mass, momentum and energy. These equations fully describe the three-dimensional dynamics of an inviscid, rotational, compressible fluid. The discretisation used is first-order accurate, cell vertex, upwind difference in space with explicit time-marching. The spatial accuracy, however, approaches second order in the final, steady-state solution. The solution is obtained in a cylindrical domain around the propeller. A permeable, non-reflective boundary condition based on the Riemann invariants is applied on the outer surface of the domain. In practice, the method can be applied to propeller flows in free streams at medium subsonic to transonic Mach numbers, and yields detailed distributions of all flow variables on the propeller surfaces as well as in the field. A typical mesh containing approximately 140,000 cells is shown in figure 2. The grid is clustered at the blade leading and trailing edges and near the blade tip.

Comparison of Computed and Measured Data for Isolated Propeller

A comparison was made between predictions using the three-dimensional compressible Euler finite-volume codes and measurements on the isolated propeller in the ONERA S1MA wind tunnel. A test matrix of six cases was chosen for comparison of integrated performance parameters. Figure 3a shows the comparison of predicted and measured thrust coefficient. Predicted thrust coefficients are between 4% and 6% higher than the measurements for the 65^0 blade pitch, and between 10 and 17% higher for the 63^0 blade pitch. This indicates that the higher loading case is better predicted, but in both cases the coefficients follow the measured gradient versus advance ratio behaviour. The predicted and measured torque and efficiency are presented in figures 4 and 5. Although the predicted and measured torque differ significantly, the trends of the data match well. In figure 5, small differences are also shown in predicted efficiency, but again the trends are well represented. It is seen that the combination of a larger torque value and slightly smaller thrust coefficient combine to give a slightly lower efficiency for the predictions.
At 63 degrees blade pitch the comparison is not as good as for the 65 degrees so that the influence of blade settings on thrust coefficient variations is underestimated.

Actuator Disk Modelling

An actuator disk is used to simulate the effect of flow through turbo-machinery rotors such as propellers, turbine and compressor blade rows. It is an artificial representation producing sudden discontinuities in the flow properties, see figure 10. An efficient procedure for the generation of actuator disk models of advanced propellers at zero angle of incidence has been developed. Several actuator disk models were generated during the course of GEMINI II.
Each model consists of the circumferentially averaged, radial variation of flow field properties, such as radial and tangential velocity components, at a specified axial station downstream of the pitch change axis. These models were used successfully by the airframe group in the aerodynamic calculations of the flow fields around fuselage-wing-nacelle and wing-nacelle power-on configurations.

CIRA code

Here, only a brief description is given; a more detailed description of the code is available in

open literature[4][5][6]. The CIRA flow solver ZEN (Zonal Euler Navier-Stokes) is a multizone code solving both Euler and RANS equations using multiblock structured grids, with the capability of simulating the slipstream induced by a propeller on the aerodynamic flow field. Different k-ε formulations and the Baldwin-Lomax turbulence models can be used to close the Navier-Stokes equations. The finite volume cell-centred scheme is used together with self-adaptive 2nd and 4th order artificial dissipation terms. The block-to-block coupling is performed in a conservative way, allowing different grid properties at block interfaces. The solution procedure is based on a time-marching strategy. An explicit multigrid method is applied together with local time stepping and implicit residual smoothing to accelerate the convergence.
Globally, the ZEN code results in a very flexible tool, validated for a large set of applications and with the capability of handling complex three-dimensional geometries.
The slipstream induced by a propeller is simulated via actuator disk boundary conditions: the jump in total pressure and temperature, together with the swirl and contraction angles can be specified at the actuator disk; a second possibility is to use the propeller force coefficients as volume force terms in the field equations Due to the zero incidence considered for the propeller computations, the actuator disk data are uniformly distributed in the disk circumferential direction, see figures 6, 7. The actuator disk models computed by ONERA and NUIG have been used for the actuator disk boundary conditions.

Procedure for Generation of Actuator Disk Models

The steps used in the procedure for the generation of the actuator disk models are as follows.
1) The three-dimensional compressible Euler finite-volume codes described above are used to predict the inviscid flow around the propeller.
2) The predicted flow field variables in the domain downstream of the blade trailing edge and extending from the hub surface to a radial distance equal to the blade tip radius, are circumferentially averaged. Simple linear averaging is used.
3) The axial location of the actuator disk is usually specified as a fraction of the blade tip radius downstream of the pitch change axis. Typical value is X/Rtip=0.2.

Linear interpolation is used in the axial direction, if needed, to find the actuator disk data. The resulting actuator disk model consists of the radial variation, at a fixed axial location, of the radial velocity component, the relative and absolute tangential velocity components, the axial velocity component and the non-dimensional total pressure and total temperature. Figure 6 and 7 show plots of non-dimensional total pressure and temperature, and of swirl and contraction angles for a typical actuator disk model of the GEMINI II isolated propeller. The model was obtained at an axial location X/Rtip=0.2, downstream of the pitch change axis. The data show a smooth variation in the radial direction. This smooth variation indicates that a sufficiently refined mesh is being used in the flow analysis.
In APIAN the non-zero inflow angle condition will be considered; then, the actuator disk data will be computed as a function of r and of the circumferential direction.

Comparison of Actuator Disk Simulations and Propeller Blades computations

A C-C grid for the Euler simulation of the isolated propeller applying the actuator disk boundary condition was generated by CASA, see figure 8. The iso-mach lines of the Euler solutions (CIRA) computed at M_∞=0.7 is shown in figure 9. It is clearly visible the effect of the actuator disk on the flow field.
In figure 10 the behaviour of the velocity components, the pressure, and the total pressure across the actuator disk is reported along a straight horizontal line at r/Rtip=0.5 in the X-Y plane. As a reference the actuator disk is indicated in figure 8, and the X-axis is reported also together with the geometry in figure 9. The discontinuity introduced by the actuator disk is visible in all the reported variables. In the X-Y plane the velocity component along the Z axis remain zero until the actuator disk that induces a specified swirl; it is worth noticing that the angle behind the actuator disk is specified via the boundary conditions but the velocity magnitude is part of the solution. The X and Y component are already not zero due to the spinner that starts at about X=900, see figure 9. The total pressure is not constant along X because we are not looking along a streamline but along a fixed horizontal line, then we are looking to particles coming from a higher loaded part of the blade (i.e. r/Rtip>0.5).
The same averaging performed for the ONERA and NUIG results to build the actuator disk model

was realised in the slipstream and the data compared with results computed by steady Euler solver (CIRA) applying the actuator disk boundary conditions. These comparisons are shown in figures 11 to 15 at a fixed X station, and precisely X/Rtip=1. Globally, the results agree fairly well. The main difference (in percentage) is noticeable, in figure 13, for the radial component of the velocity. Such disagreement is partially due to a different geometrical representation of the spinner and of the minimum body used for the three calculations. Furthermore, it is quite understandable that in the approximation of the actuator disk the radial component is different from that computed by simulating the real blade shape (NUIG, ONERA). Anyhow, the relative importance of the radial velocity component is negligible with respect to the other two. The same agreement has been found at other X stations. Then we can draw the following conclusions: the procedure here used to build numerically the actuator disk data is working correctly; the slipstream induced by the actuator disk boundary condition well reproduces that computed when using the pseudo-unsteady codes. This allows us to use with confidence the actuator disk approach when computing the flow field around complex configuration (full aircraft) in order to compute the aerodynamic propulsion airframe interaction.

Wing Installation Effects

The interaction between propeller, wing and nacelle is accounted for analysing the interaction effect on propeller performance and consequently improve the actuator data provided to airframe-aerodynamic group.

The two domains decomposition, see figure 1, is aimed at computing the mutual interaction between propeller and wing or nacelle. Hence we have a rotating domain for the propeller (150,000 points) and a fixed domain for the wing domain (124,500 points). For this application some modifications of CANARI code have been done and a specific boundary condition has been developed. At the interface between domains with different rotating velocities the new boundary condition allows the transmission of the tangential averaged flow values upstream and downstream through the two domains interface. A grid constraint on the interface is to have an axis-symmetrical surface with identical radial position of the nodes for the two domains. The averaged values in tangential direction are computed by line-averaging without interpolation. The radial distribution of averaged static pressure on the interface boundary in the downstream domain is used as exit condition of the upstream domain, with respect to compatibility relations. The tangential averaged values of the total pressure, the total temperature and the velocity components - in a cylindrical coordinate system (V_x,V_r,V_θ,) - are computed on the exit boundary of the upstream domain and used as inflow condition for the downstream domain.

The propeller conditions used for this simulation are the cruise conditions of GEMINI II. The geometry was simplified for the wing and the nacelle in order to have an axis-symmetrical interface between the rotating part and the fixed domain. In figure 16 relative Mach numbers contours are plotted on the propeller domain and the absolute Mach number on the wing domain. We can see the acceleration on the upper side of the port-board wing due to the slipstream of the propeller which is rotating clockwise, view from the back.

The increase of the thrust coefficient DCT due to the installation effect is plotted versus the advance ratio in figure 3b). The computed increase of the thrust coefficient DCT is comparable with the results of ONERA S1MA test campaign.

Airframe Aerodynamic Analysis

Fuselage-wing-nacelle configuration

The numerical results discussed here were produced at CIRA, using the Alenia grid [4] and the CIRA flow solver ZEN [5],[6]. A short description of ZEN is in the related section above.

In figure 18 a view of the surface grid is presented; the complete grid is made of 233 blocks and consists of 1.5 million points. The geometry corresponds to half wind tunnel model.

A large set of computations was realised during the GEMINI II project:

- Mach = 0.68, 0.7, 0.72; α = 0, propeller off;
- Mach = 0.7; α = 1, propeller off;
- Mach = 0.7; α = –1, 0, 1; propeller on;
- Mach = 0.5; α = 0,1; propeller on/off.

Some of these conditions were considered for both the port and the starboard wing.

These tests were made before the wind tunnel campaign, so that a real life "blind numerical testing" was performed.

Here, some conclusions of the analysis are described, and a selection of results is shown.

In figure 17 the location of the wing sections instrumented with the pressure taps are indicated.

Nacelle Redesign in GEMINI

The first numerical analysis (e.g CIRA, Alenia) of the airframe model with the original nacelle, that ended before the trailing edge of the lower side wing, gave a clear indication of separation of the flow field in the rear part of the nacelle already at M=0.4, $\alpha=1^{\circ}$.

On the base of this indication a new nacelle has been designed by Aerospatiale, and a new grid generated by Alenia. The design was anyway limited by a number of already fixed parameters, so that also the new nacelle shape showed a separation in the experiments.

Guide Lines to Wind Tunnel Test Matrix

The numerical results gave clear indications of the expected flow field patterns (Cp distributions, shocks appearance, possibly separated areas, etc.) that were useful during the refinement of the wind tunnel test matrix and during the experiments as a reference for the incoming data.

A special effort was dedicated at CIRA to estimate the buffet onset limit of the complete configuration. This information was used to eliminate some incidences initially foreseen, and during the experimental buffet survey was considered as the border of the critical pattern.

Numerical Experimental Correlation

The overall comparison of numerical and experimental pressure distribution along the wing span is rather satisfactory even if the lift has not been fitted in calculations; see figures 20-23,and 26. Furthermore, the computational results in figures 20 to 24 are for $\alpha=1$(deg), while the experimental α is equal to 0.7 (deg).

The numerical shocks are generally stronger and located more downstream than the experimental ones, this is a consequence of the inviscid model adopted and of the fact that circulation was not fitted. As expected, due to the inviscid model and to the relatively low Reynolds number achieved in the experiments, the numerical rear pressure recovery is higher than the experimental one. As far as the wing sections close to the nacelles, see figure 21, it is worth to stress that in the wind tunnel experiments, large separations have been seen in the rear part of the outer and inner side of the nacelle. In the Euler simulations a supersonic area followed by a shock was found near the rear part of the intersection between the nacelle and the lower surface of the wing. Then, a meaningful difference can be seen between the numerical and experimental data on the lower side of the wing.

The slipstream induced by the actuator disk model well reproduces the effects of the propeller on both port and starboard wing; see figures 22, 23, and 25.

A strong slipstream influence has been found; in fact the pressure distribution is affected from the half-span vertical plane until about the 60% of the wing, see figure 19. The rear loading is not influenced by the slipstream.

The numerical and experimental pressure distributions agree nicely on a large portion of the nacelles. On the lower side the accordance is very good, see figure 24; a difference is visible in the aft part where separation occurs.

Some discrepancies are found in the lift coefficients. This is partially justified by the use of the Euler equations and are consistent with the differences found for the pressure coefficient on the wing. The power effect on the lift, both in the wind tunnel and numerical testing, seems not to be in accordance with what verified in other similar configurations. We might say that this is due to a strong installation interference between the nacelle, the wing and the fuselage magnified by the compressibility of the flow field.

CIRA results are also compared to those produced by DASA-Dornier. They correlate very well for propeller off conditions; some small discrepancies are present for the peaks and the shock definition. For propeller on conditions globally the results agree fairly well, see figure 20, (e.g the differences being similar to the propeller off case), except for the wing sections, both on the port and starboard wing, down-washed by the propeller slipstream, see figure 21. In these sections, some discrepancies of the adopted actuator disk model are inducing a different slipstream.

Wing-Nacelle Configuration

In the new project APIAN one of the model enhancements is the redesign of the nacelle. In fact, the nacelle designed within GEMINI II is showing a separation in the wind tunnel experiments that introduces spurious drag and noise. Before the new nacelle construction a theoretical analysis of its aerodynamic behaviour is being accomplished. In order to speed up this process it was decided to consider a simplified geometrical model with respect to the wing-nacelle-fuselage configuration: the nacelle was mounted on the theoretical wing including the wing-nacelle fillet and eliminating the fuselage (see figure 27). This is justified by the fact that the focus is on the nacelle aerodynamics and by

the consideration that the fuselage interference with the nacelle behaviour is relatively negligible. Furthermore, in the following of the APIAN project the full configuration will be considered allowing an evaluation of the fuselage aerodynamic interference. Potential, Euler and Navier-Stokes computations have been performed on this geometry. An overview of the Euler grid is show in figures 28 and 29; this mesh has been generated using the ICEM CFD code and contains about 900.000 grid points. The topology of the grid is relatively complex: an external H-H is used, around the nacelle a O-O is applied. During the mesh generation many blocks have been used (more then one hundred), but before running the flow solver large sets of blocks have been merged. A discussion of these results will be presented at the conference; here only preliminary results are reported in figures 30 and 31.

Conclusions

A wide range of CFD simulations related to propulsion airframe integration for propeller driven aircraft flying at transonic speed has been presented. The capability of analysing these problems with sufficient engineering accuracy has been assessed. The low Reynolds number achieved in the wind tunnel testing gives a pessimistic comparison between the inviscid calculations and the experiments. The numerical experimental comparisons shown are not a basis for judging the accuracy for the Euler solvers. Looking for Euler analysis at given lift/thrust values is a much better basis for design tasks. Navier-Stokes simulations improves the correlation albeit at the expenses of increased difficulties and costs.

A completely numerical simulation procedure going from the aerodynamic analysis of isolated propellers up to wing installation effects on the propeller, and finally to the analysis of the slipstream-airframe interaction has been successfully tested.

The performed aerodynamic analysis gave a good indication of loads (both on the blades and on the airframe), propeller-to-airframe interaction, lift/thrust coefficient trends, and was very useful in supporting wind tunnel model preparation and wind tunnel testing.

A synergetic use of numerical and experimental tools has been achieved in the described research projects.

Further viscous and unsteady, aerodynamic analyses will be performed within the APIAN project and compared with the new wind tunnel tests data that will include boundary layer and PIV measurements.

Acknowledgements

The authors wish to acknowledge: Prof. B.Wagner, for the useful discussions during the numerical/experimental correlation performed within GEMINI II, and for allowing the use of the DASA-Dornier results; the project leader C.Castan, for the precious co-ordination of the work that brought GEMINI II to the success; P.Vitagliano (Alenia) for providing the Euler grid for the complete GEMINI II model; A.Abbas (CASA) for providing the Euler grid for testing the actuator disk; the project team; and CIRA for supporting the work.

References

1. C.Castan, A.Dumas, "Aerodynamic Integration of High Speed Propeller on Aircraft Recent Investigations in european Wind tunnels", to be presented at 21st ICAS, 13th-18th September, 1998.

2. A. M. Vuillot, V. Couailler and N. Liamis "3-D Turbomachinery Euler and Navier-Stokes Calculations with a multidomain cell-centered approach." AIAA Paper 93-2576 (ONERA ref. TP 1993-106) AIAA/SAE/ASEE 29th Joint Propulsion Conference and Exhibit, Monterey, Ca. (USA),June 28-30 1993.

3. Quinlan, N.J.,"A Computational Mthod for Aerodynamic Analyses of Propellers", MEngS Thesis, National University of Ireland, 1994.

4. M.Amato, P.Catalano (CIRA) and B. Wagner (DORNIER), "Experimental Numerical Comparison for the GEMINI II Complete Configuration", XIV Congresso AIDAA, Napoli 20-24 ottobre 1997.

5. A.Amendola, R.Tognaccini, J.W.Boerstoel, A. Kassies, "Validation of A Multiblock Euler Solver with Propeller-Slipstream Flows", AGARD Conference Proc. No. 437 , 1987.

6. M.Amato, G.Iaccarino, L.Paparone, "Adaptive Local Grid Refinement for Multiblock Solvers" ICAS, 20th Congress, Sorrento (NA), Italy, 8-13 September, 1996.

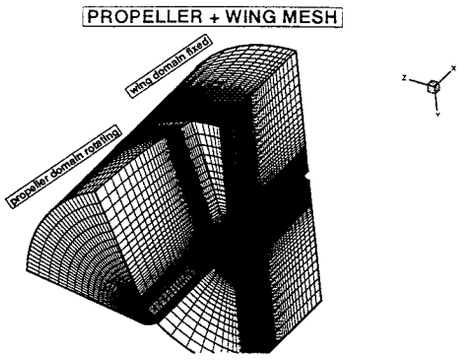

Figure 1 - Grid around the wing-propeller configuration

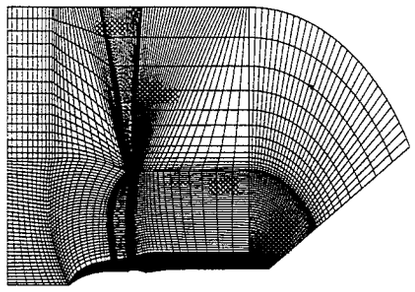

Figure2 - UCG grid around the isolated propeller

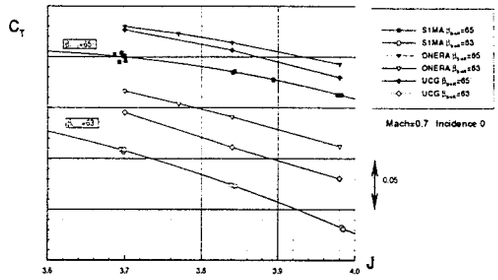

3a) - Comparison of measured with computed total force for the GEMINI II isolated propeller

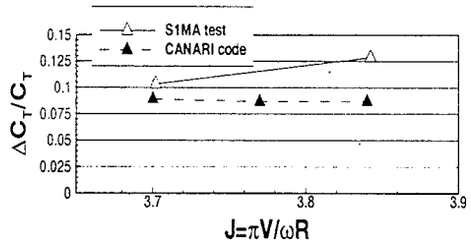

3b) - Comparison of measured with computed total force for the wing-propeller configuration

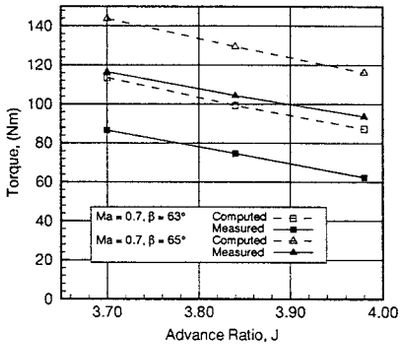

Figure 4 - Comparison of measured with computed torque for the GEMINI II isolated propeller

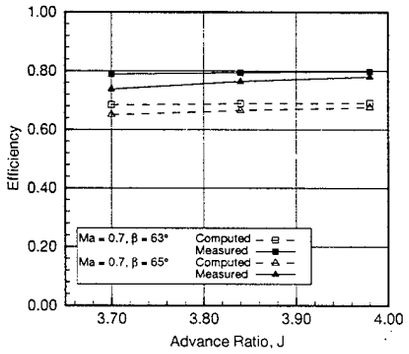

Figure 5 - Comparison of measured with computed efficiency for the GEMINI II isolated propeller

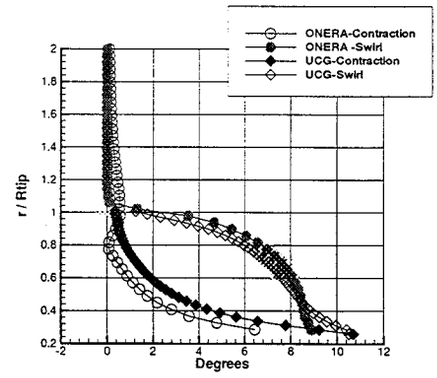

Figure 6 - Contraction and Swirl vs. R at the actuator disk station for the GEMINI II isolated propeller

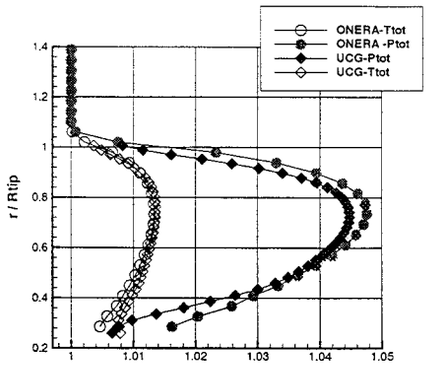

Figure 7 - Predicted variation of total pressure and total temperature vs. R at the actuator disk station for the GEMINI II isolated propeller

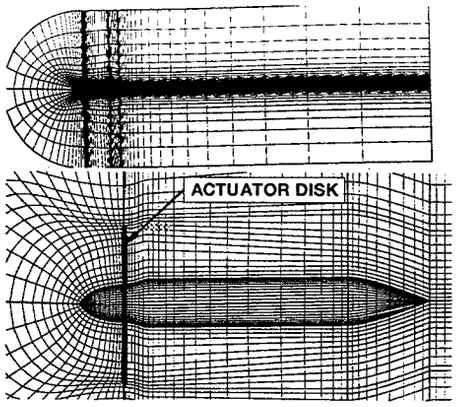

Figure 8 - Grid around the isolated propeller configuration

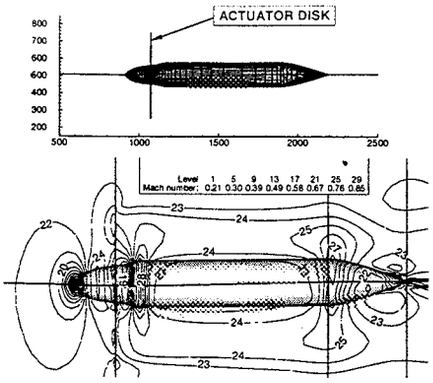

Figure 9 - Isolated propeller configuration and iso-mach lines

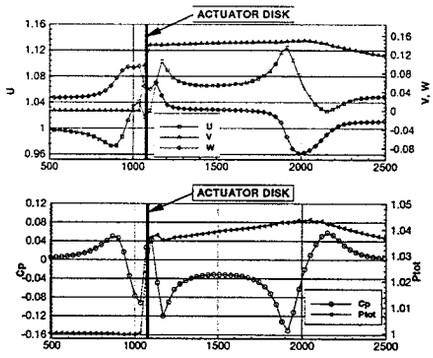

Figure 10 - Velocity components, Pressure, and Total Pressure across the Actuator Disk at r/Rtip=0.5

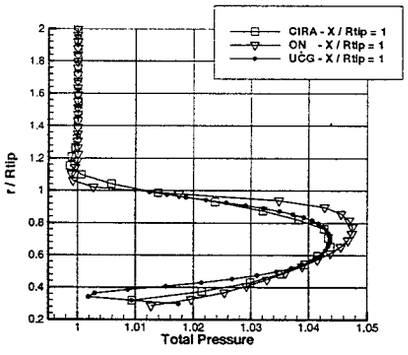

Figure 11 -Total Pressure Comparison at X/Rtip=1

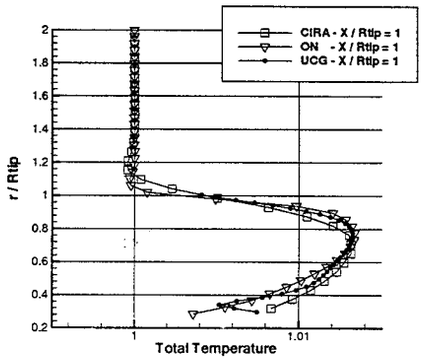

Figure 12 - Total Temperature Comparison at X/Rtip=1

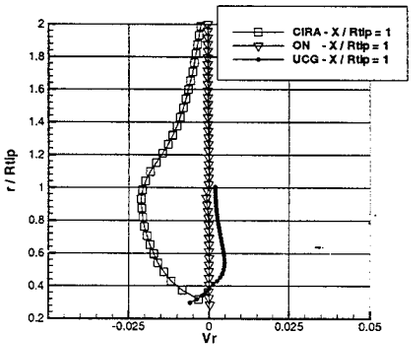

Figure 13 - Radial velocity comparison at X/Rtip=1

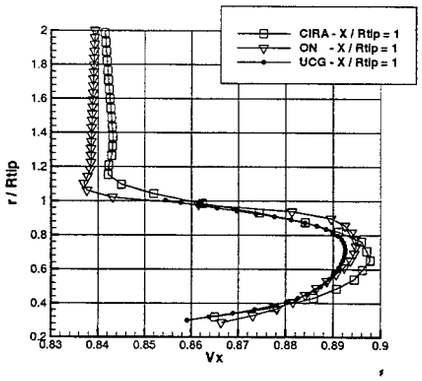

Figure 14 - Axial velocity comparison at X/Rtip=1

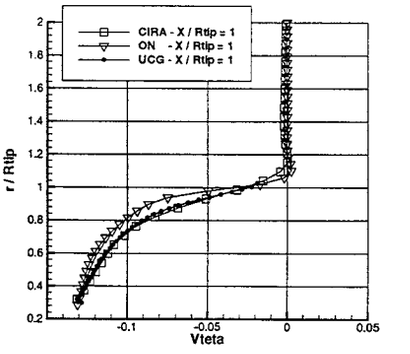

Figure 15 - Tangential velocity comparison at X/Rtip=1

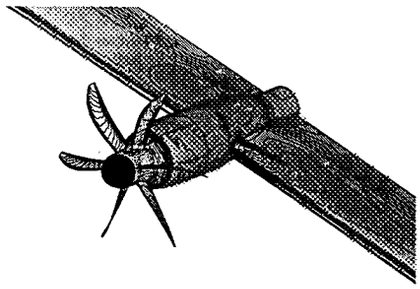

Figure 16 - Iso-mach contour lines on the wing propeller surface

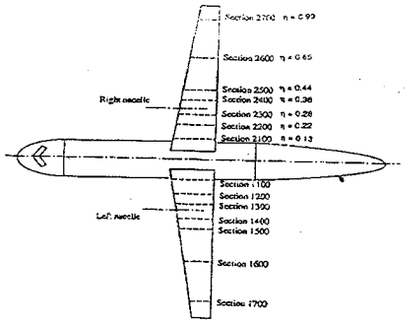

Figure 17 - Wing Sections instrumented with pressure taps

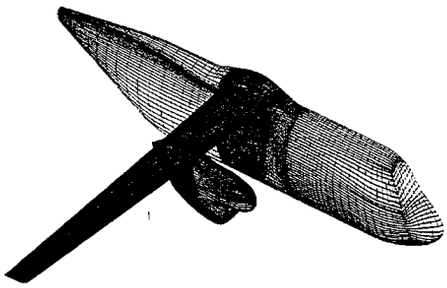

Figure 18 - Surface Grid for the complete airframe

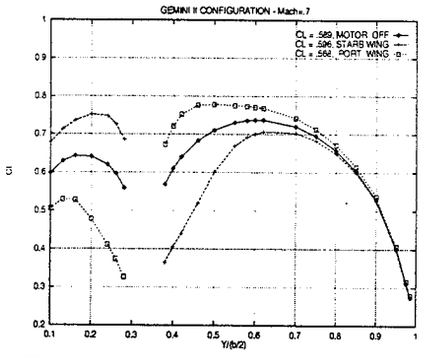

Figure 19 - Computed span-wise lift distribution

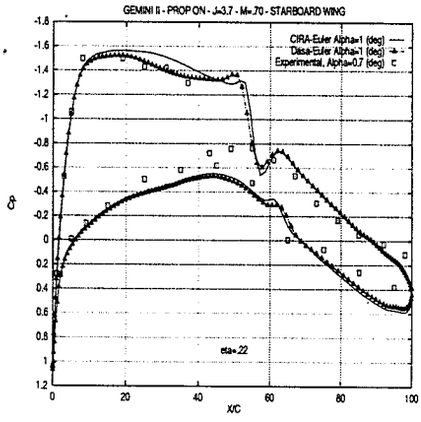

Figure 20 - Cp at η=.22 M=0.7, prop on, CFD-α=1, EXP- α=0.7. Starboard Wing

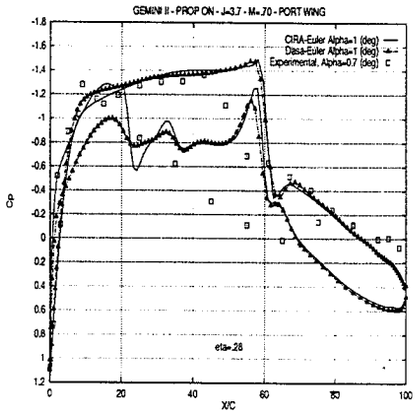

Figure 21 - Cp at η=.28 M=0.7, prop on, CFD-α=1, EXP- α=0.7, Port Wing

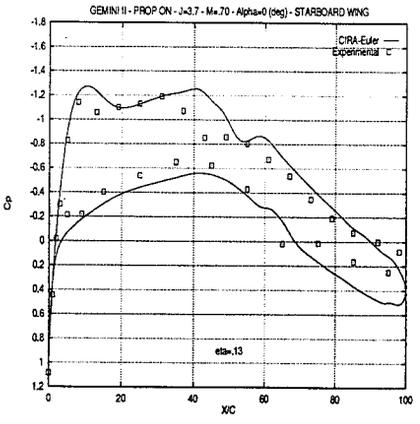

Figure 22 - Cp at η=.13 M=0.7, prop on, CFD-α=0, EXP- α=0, Starboard Wing

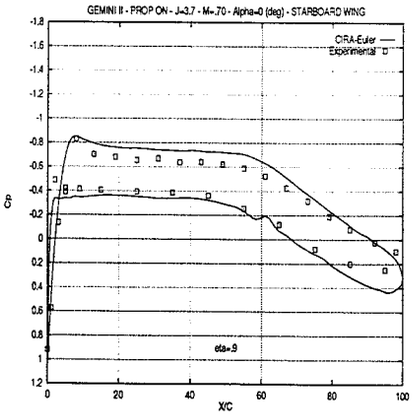

Figure 23 - Cp at η=.9 M=0.7, prop on, CFD-α=0, Port Wing

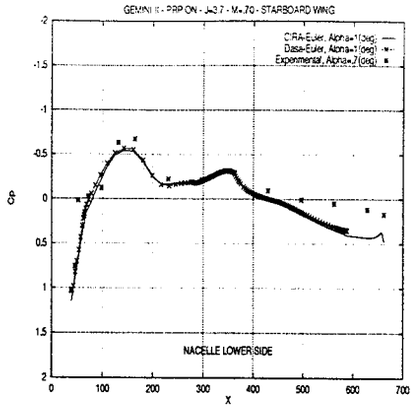

Figure 24 - Cp at M=0.7, prop on, CFD-α=1, EXP- α=0.7, Nacelle Lower Middle Section

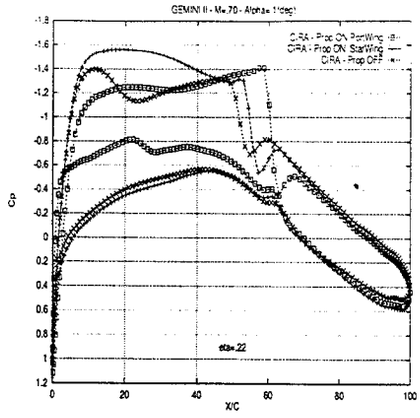

Figure 25 - Cp at η=.22 M=0.7, CFD-α=1 Slipstream effect

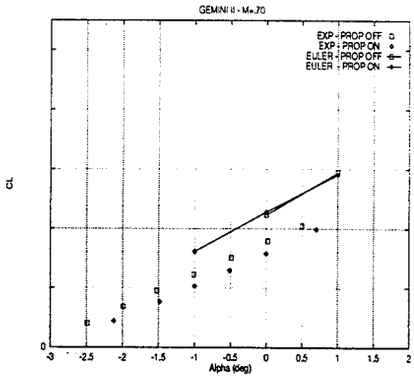

Figure 26 - Lift vs. α plot

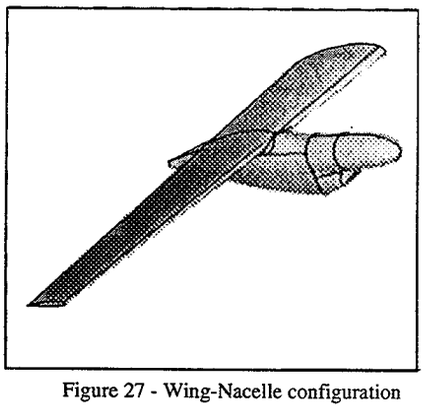

Figure 27 - Wing-Nacelle configuration

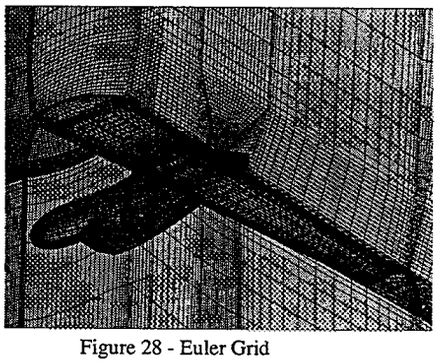

Figure 28 - Euler Grid

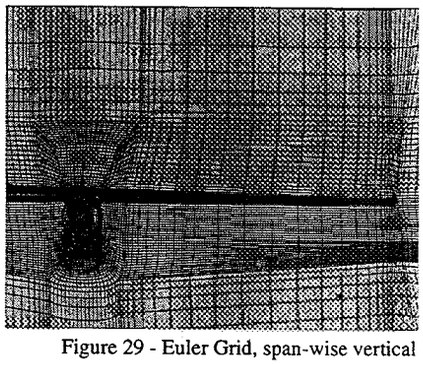

Figure 29 - Euler Grid, span-wise vertical coordinate grid plane

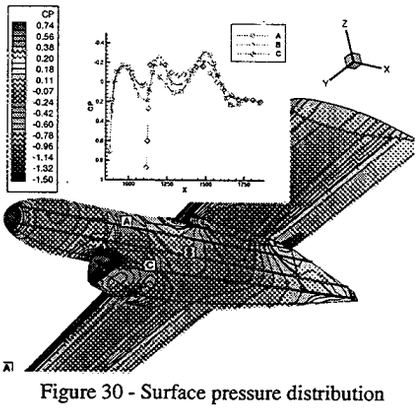

Figure 30 - Surface pressure distribution

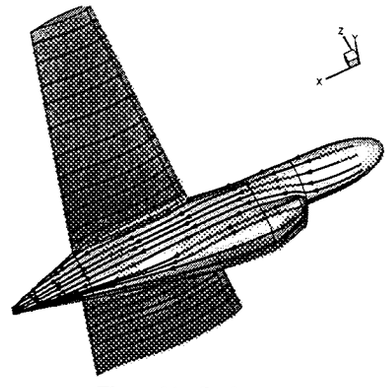

Figure 31 - Surface streamlines